Couette-Taylor instability in viscoelastic fluids

B. J. A. Zielinska*
Laboratoire de Physique Théorique, Université de Nice, Parc Valrose, 06034 Nice Cédex, France

Y. Demay
Laboratoire de Mathémathiques, Université de Nice, Parc Valrose, 06034 Nice Cédex, France
(Received 8 February 1988)

We study the Couette-Taylor instability for a large class of Maxwell models. We find that for a wide range of parameters the basic equations do not have an axisymmetric Couette-like solution. Furthermore, we show that from Maxwell-type models oscillatory instability is not to be expected at threshold. We calculate the critical Reynolds number and the critical wave vector by integrating the perturbation equations numerically for the cases of small and large gap.

I. INTRODUCTION

Many fluids made of large macromolecules exhibit unusual properties as compared to fluids made of small molecules.[1-3] These fluids are commonly called the viscoelastic fluids because they posses viscous properties typical for fluids, next to some elastic properties typical for solids. These fluids have many applications in polymer processing and therefore it is important to study their properties, in particular under flow conditions.

Among the unusual properties are the shear-rate–dependent viscosity[4] and the so-called Weissenberg effect[5-7] (the fluid climbs a fast turning rod instead of being pushed away from it). But perhaps the most characteristic is the recoil effect.[8,9] The fluid recoils partially to its previous state. The memory of the previous state is fading, however: the longer the fluid stays in its new state, the less it recoils. This effect points to existence of a characteristic time for memory. The simplest rheological expression for stress tensor which captures both the viscosity and elasticity is the so-called Maxwell model:[10]

$$\vec{\vec{\Sigma}}+t_0\frac{\partial\vec{\vec{\Sigma}}}{\partial t}=\eta(\delta\vec{V}+\nabla\vec{V}^{\dagger}) . \tag{1.1}$$

Here $\vec{\vec{\Sigma}}$ is the stress tensor, $\nabla\vec{V}+\nabla\vec{V}^{\dagger}$ is the rate of strain tensor ($\vec{V}$ is the velocity field and $\nabla\vec{V}^{\dagger}$ denotes the transposed of $\nabla\vec{V}$), t_0 is the characteristic time for memory, and η is the viscosity. Note that for $t_0=0$, Eq. (1.1) describes the usual Newtonian fluid. Equation (1.1) forms a basis for many rheological equations of state for the stress tensor existing in the literature.

The purpose of this work is to study the properties of a large class of Maxwell models for viscoelastic fluids under shear flow between rotating cylinders, the so-called stability analysis of the steady state subject to perturbations of the form of Taylor vortices. The results are given in Sec. V and conclusions in Sec. VI.

II. THE SYSTEM

We consider the Taylor system consisting of viscoelastic fluid contained between concentric cylinders with radii R_1 and R_2 ($R_1<R_2$) of infinite length and rotating with angular velocities Ω_1 and Ω_2, respectively. Let us denote the velocity field in cylindrical coordinates by $\vec{V}=(V_R,V_\theta,V_Z)$ and the stress tensor by $\vec{\vec{\Sigma}}$. The flow of the fluid is governed by the Navier-Stokes equation together with the incompressibility condition:

$$\rho\frac{d\vec{V}}{dt}=\mathrm{div}(\vec{\vec{\Sigma}})-\nabla p , \tag{2.1a}$$

$$\mathrm{div}(\vec{V})=0 , \tag{2.1b}$$

where ρ is the density of the fluid and p is the hydrostatic pressure. For the pressure tensor $\vec{\vec{\Sigma}}$ we will use the constitutive relation given in Eq. (1.2).

In order to reduce the number of parameters we put Eqs. (1.2) and (2.1) into dimensionless form by the following scaling rules:

$$\begin{aligned} &r=\frac{R}{R_1},\quad z=\frac{Z}{R_1},\quad s=t\Omega_1,\\ &\vec{v}=\frac{\vec{V}}{\Omega_1R_1},\quad \vec{\vec{T}}=\frac{\eta}{\rho^2R_1^4\Omega_1^3}\vec{\vec{\Sigma}} ,\\ &\Gamma=\Omega_1t_0,\quad \mathcal{R}=\frac{\rho R_1^2\Omega_1}{\eta},\quad a=\frac{R_2}{R_1} ,\\ &q=\frac{1}{\rho R_1^2\Omega_1^2}p,\quad \omega=\frac{\Omega_2}{\Omega_1} . \end{aligned} \tag{2.2}$$

Equations (1.2) and (2.1) now become

$$\begin{aligned} \vec{\vec{T}}+\Gamma\Big[&\frac{d\vec{\vec{T}}}{ds}+\tfrac{1}{2}[\vec{\vec{T}}\cdot(\nabla\vec{v}-\nabla\vec{v}^{\dagger})-(\nabla\vec{v}-\nabla\vec{v}^{\dagger})\cdot\vec{\vec{T}}]\\ &+\tfrac{1}{2}A[\vec{\vec{T}}\cdot(\nabla\vec{v}+\nabla\vec{v}^{\dagger})+(\nabla\vec{v}+\nabla\vec{v}^{\dagger})\cdot\vec{\vec{T}}]\Big]\\ &=\nabla\vec{v}+\nabla\vec{v}^{\dagger} , \end{aligned} \tag{2.3a}$$

$$\mathrm{div}(\vec{v})=0 , \tag{2.3b}$$

$$\frac{d\vec{v}}{ds}=-\nabla q+\mathcal{R}^{-1}\mathrm{div}(\vec{\vec{T}}) , \tag{2.3c}$$

subject to the boundary conditions,

$$v_r = v_z = 0 \text{ at } r = 1 \text{ and } r = a \ ,$$

$$v_\theta = 1 \text{ at } r = 1, \text{ and } v_\theta = wa \text{ at } r = a \ .$$

III. STEADY-STATE SOLUTION

For small enough angular velocities Eqs. (2.3) have an axisymmetric steady-state solution depending only on the distance to one of the cylinders. Therefore we seek velocity field, stress tensor, and pressure of the form:

$$\vec{v} = (0, v_\theta^0(r), 0), \quad \overleftrightarrow{T} = \overleftrightarrow{T}^0(r), \text{ and } q = q^0(r) \ .$$

It is shown in Appendix A that v_θ^0 fulfills the following differential equation:

$$\left[\frac{d}{dr} + \frac{2}{r}\right]\left[\frac{\dfrac{dv_\theta^0}{dr} - \dfrac{v_\theta^0}{r}}{1 + \Gamma^2(1 - A^2)\left[\dfrac{dv_\theta^0}{dr} - \dfrac{v_\theta^0}{r}\right]^2}\right] = 0 \ . \tag{3.1}$$

It can be checked that the solution of this equation has the following form (for details see Appendix A):

$$v_\theta^0(r) = \frac{\lambda r^3}{2\Gamma\sqrt{1-A^2}}\left[r^2 - \left[\frac{r^4\lambda^2}{\Gamma^2(1-A^2)} - 1\right]^{1/2} - \Gamma\sqrt{1-A^2}\arctan\left[\frac{r^2\lambda^2}{\Gamma^2(1-A^2)} - 1\right]^{1/2} + \mu\right] , \tag{3.2}$$

where we have chosen the branch of the solution corresponding to the classical Couette flow for $A = \pm 1$. The two constants λ and μ appearing in solution (3.2) are chosen to verify the boundary conditions $v_\theta^0(1) = 1$ and $v_\theta^0(a) = \omega a$. These boundary conditions cannot always be satisfied for any $-1 < A < 1$. Its existence region corresponds to the range of values of A, Γ, and λ for which the square roots appearing in solution (3.2) remain real. The region of existence of v_θ^0 for $a = 1.0526$ and $a = 1.33$ as a function of the relevant parameter $\Gamma(1-A^2)^{1/2}$ is shown in Fig. 1. In this figure one can see that the region of existence opens up to very large values of v_θ^0 in the limit $A \to \pm 1$ or $\Gamma \to 0$. In both limits the steady flow becomes the classical Couette flow. Consequently, for a large range of $\Gamma(1-A^2)^{1/2}$ Eqs. (2.3) do not have a steady axisymmetric solution.

In Appendix A we also calculate the elements of the stress tensor for the steady state and obtain

$$\begin{aligned} T_{rr}^0 &= -\Gamma(1+A)\left[\frac{dv_\theta^0}{dr} - \frac{v_\theta^0}{r}\right]T_{r\theta}^0 \ , \\ T_{\theta\theta}^0 &= \Gamma(1-A)\left[\frac{dv_\theta^0}{dr} - \frac{v_\theta^0}{r}\right]T_{r\theta}^0 \ , \\ T_{r\theta}^0 &= \frac{\dfrac{dv_\theta^0}{dr} - \dfrac{v_\theta^0}{r}}{1 + \Gamma^2(1-A^2)\left[\dfrac{dv_\theta^0}{dr} - \dfrac{v_\theta^0}{r}\right]^2} \ , \end{aligned} \tag{3.3}$$

and

$$T_{rz}^0 = T_{\theta z}^2 = T_{zz}^0 = 0 \ .$$

The experimentally important ratio N_2/N_1 of secondary to primary normal stress difference is in our case defined by $N_2 = T_{rr} - T_{zz}$ and $N_1 = T_{\theta\theta} - T_{rr}$. This ratio varies drastically as function of A. Using Eq. (3.3) it is easy to see that for $A = -1$ (the upper convective deriva-

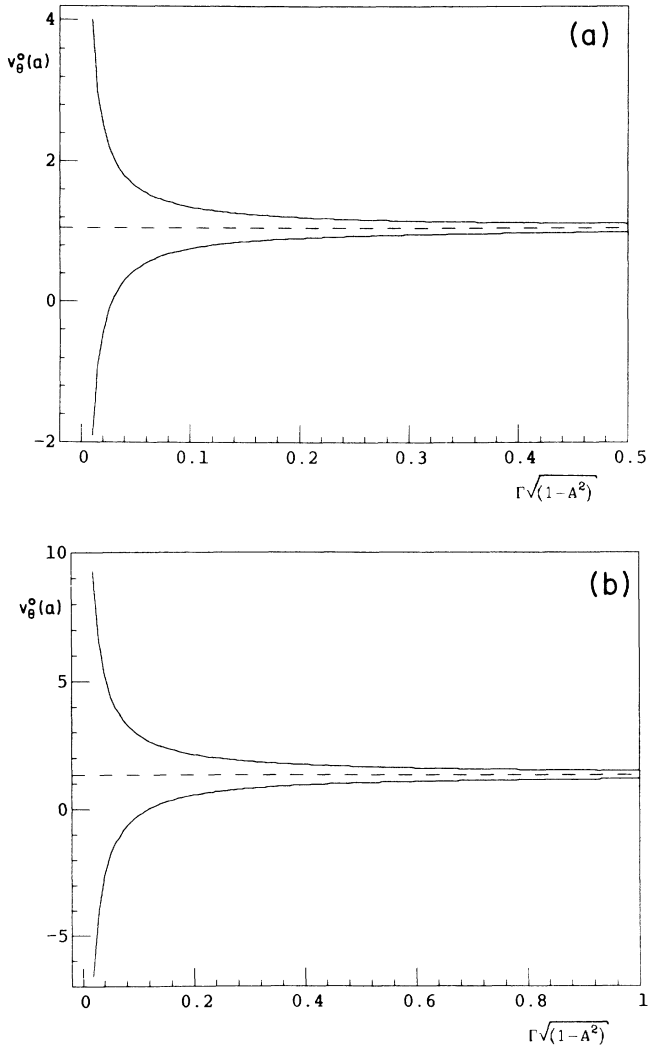

FIG. 1. Region of existence of the axisymmetric solution of the basic equations v_θ^0 for (a) $a = 1.0526$ and (b) $a = 1.33$.

tive) $N_2/N_1=0$, for $A=0$ (the fully corotational model) $N_2/N_1=-0.5$, and for $A=1$ (the lower convective derivative) $N_2/N_1=-1$. The range of N_2/N_1 observed experimentally lies between 0 and -0.5,[13,20] so we can conclude for the physically realistic models that A will have a value between -1 and 0.

IV. STABILITY ANALYSIS

In this section we study the stability of the steady state subject to perturbations of the form of Taylor vortices. It can be shown using the symmetry arguments that the perturbations around the stationary state will have the following form:[24]

$$\begin{aligned}\vec{v}(r,\theta,z)&=\vec{v}^{\,0}(r)+[\vec{u}(r)e^{\sigma t+im\theta+i\alpha z}+\text{c.c.}]\ ,\\ \overleftrightarrow{T}(r,\theta,z)&=\overleftrightarrow{T}^{\,0}(r)+[\overleftrightarrow{\eta}(r)e^{\sigma t+im\theta+i\alpha z}+\text{c.c.}]\ ,\\ q(r,\theta,z)&=q^0(r)+[\psi(r)e^{\sigma t+im\theta+i\alpha z}+\text{c.c.}]\ ,\end{aligned}\tag{4.1}$$

where $\sigma\in\mathbb{C}$, $m\in\mathbb{Z}$, $\alpha\in\mathbb{R}$, and c.c. denotes the complex conjugate.

Substituting the expressions (4.1) into Eqs. (2.3) and linearizing in the perturbations we obtain a set of differential equations for the components of $\vec{u}(r),\overleftrightarrow{\eta}(r)$, and for $\psi(r)$ (for details see Appendix B). These equations have to be solved with the boundary conditions:

$$u_r(1)=u_\theta(1)=u_z(1)=0\ ,$$
$$u_r(a)=u_\theta(a)=u_z(a)=0\ .$$

As shown in Appendix B the differential equations can be written in the following form:

$$\frac{d}{dr}\begin{bmatrix}u_r\\u_\theta\\u_z\\\eta_{r\theta}\\\eta_{rz}\\\psi\end{bmatrix}=\mathcal{M}(r,\sigma,m,\alpha,a,\omega,\mathcal{R},\Gamma,A)\begin{bmatrix}u_r\\u_\theta\\u_z\\\eta_{r\theta}\\\eta_{rz}\\\psi\end{bmatrix}\ ,\tag{4.2}$$

where the components of matrix $\mathcal{M}$ depend explicitly on r but do not contain derivatives with respect to r. Using arbitrary boundary conditions for $\eta_{r\theta}$, η_{rz}, and ψ at $r=1$ it is possible to construct a solution satisfying

$$u_r(1)=u_\theta(1)=u_z(1)=0 \text{ and } u_r(a)=u_z(a)=0\ .$$

The value of u_θ at $r=a$ defines a function F:

$$F(\sigma,m,\alpha;a,\omega,\mathcal{R},\Gamma,A)=u_\theta(a)\ .$$

If σ, m, and α are such that $F=0$ then the functions u_r, u_θ, u_z, $\eta_{r\theta}$, η_{rz}, and ψ are eigenfunctions and σ is an eigenvalue. The differential equations (4.2) can then be solved numerically[25] using a fourth-order Runge-Kutta method and the values of F can be calculated such that:

$$F(\sigma,m,\alpha;a,\omega,\mathcal{R},\Gamma,A)=0\tag{4.3}$$

using the Newton-Raphson method.

We seek the values of $\mathcal{R}$ for which the steady state becomes unstable, that is, for $\text{Re}(\sigma)=0$. We shall distinguish two cases, with $\text{Im}(\sigma)=0$ and with $\text{Im}(\sigma)=\pm\nu$, corresponding to the onset of stationary and oscillatory instability. In the case $\text{Im}(\sigma)=0$ we have also $m=0$ and the critical value of $\mathcal{R}$ is found by minimizing it with respect to the wave vector α:

$$\frac{\partial\mathcal{R}_c}{\partial\alpha}(\alpha_c,a,\omega,\Gamma,A)=0\ .\tag{4.4}$$

In this case the function F defined by Eq. (4.3) is real and the critical parameters $\mathcal{R}_c$ and α_c can be found by solving

$$F(0,0,\alpha_c;a,\omega,\mathcal{R}_c,\Gamma,A)=0\ ,\tag{4.4a}$$

$$\frac{\partial F}{\partial\alpha}(0,0,\alpha_c;a,\omega,\mathcal{R}_c,\Gamma,A)=0\ .\tag{4.4b}$$

In the case of oscillatory instability, i.e., $\text{Im}(\sigma)=\nu$ we have similar conditions for the $\mathcal{R}_c$:

$$\frac{\partial\mathcal{R}_c}{\partial\alpha}(i\nu_c,m,\alpha_c;a,\omega,\Gamma,A)=0\ .\tag{4.5}$$

Here the function F is complex and $\mathcal{R}_c$, α_c, and ν_c are the solutions of the equations[25]

$$F(i\nu_c,m,\alpha_c;a;\omega,\mathcal{R}_c,\Gamma,A)=0\ ,\tag{4.6a}$$

$$\text{Re}\left[\frac{\partial F}{\partial\alpha}(i\nu_c,m,\alpha_c;a,\omega,\mathcal{R}_c,\Gamma,A)\times\frac{\overline{\partial F}}{\partial\sigma}(i\nu_c,m,\alpha_c;a,\omega,\mathcal{R}_c,\Gamma,A)\right]=0\ ,\tag{4.6b}$$

where the bar over the second derivative denotes the complex conjugate.

V. RESULTS

We have performed the stability analysis of the steady-state solution in the case of a rotating inner cylinder, i.e., $\omega=0$. In the case of corotating cylinders ($\omega>0$) no qualitative changes with the $\omega=0$ case is to be expected. For counterrotating cylinders ($\omega<0$), and ω sufficiently negative, there is an oscillatory instability at threshold for Newtonian fluids. One could therefore expect an interaction between this time-dependent mode and the oscillatory mode due to viscoelasticity in this region.

We have calculated the critical parameters for various values of A and Γ in the region of existence of the steady flow for two values of the gap: $a=1.0526$ (small gap) and for $a=1.33$ (large gap). In both cases the results are qualitatively similar.

The results for $\mathcal{R}_c$ as a function of the characteristic time Γ for various values of A are summarized in Figs. 2(a) and 2(b). In these figures the solid lines correspond to the stationary instability [$\text{Im}(\sigma)=0$ and $m=0$], while the dashed lines correspond to the oscillatory instability [$\text{Im}(\sigma)=\nu$ and $m=1$]. The case $A=-1$ has been studied previously[14,15,26] in the small-gap approximation.

These authors obtained a decrease of the critical Reynolds number as a function of viscoelasticity. The case $A=1$ has also been studied[16] (in the small-gap approximation) and contrary to the previous case, an increase of the critical Reynolds number as a function of viscoelasticity was obtained. These results are in qualitative agreement with our results. As it was found before in the small-gap approximation,[15] for $A=-1$ and Γ large enough, there is oscillatory instability at threshold. The crossing point of the stationary and oscillatory instability is at $\Gamma=0.17$ for $a=1.0526$ and at $\Gamma=0.45$ for $a=1.33$. For all other values of A shown in Figs. 2(a) and 2(b) there is no oscillatory instability at threshold. The oscillatory line lies always above the stationary one and the distance between them increases with increasing Γ. The experimental data[17–22] show that in most cases the critical Reynolds number increases with viscoelasticity. However, in some cases a decrease in Reynolds number has also been reported. Since in the case $A=-1$, $\mathcal{R}_c$ is, contrary to experimental data, monotonically decreasing function of Γ; it should be therefore considered as physically unrealistic model of viscoelastic fluid. We can therefore conclude that the Maxwell-type models do not predict oscillatory instability at threshold.

For $A=1$ (or -1), $\mathcal{R}_c$ is a monotonically increasing (or decreasing) function of Γ. As can be seen in Figs. 2(a) and 2(b) for intermediate values of A, $\mathcal{R}_c$ has a maximum at some value of Γ. The position of this maximum varies strongly with A and is smaller for A negative. For all values of $-1<A\leq 1$ the steady flow is stabilized for small enough Γ. The instability curves for intermediate values of A do not continue to larger Γ, because the steady-state flow does not exist in this region.

The behavior of the critical wave vector α_c as a function of the characteristic time Γ is shown in Figs. 3(a)

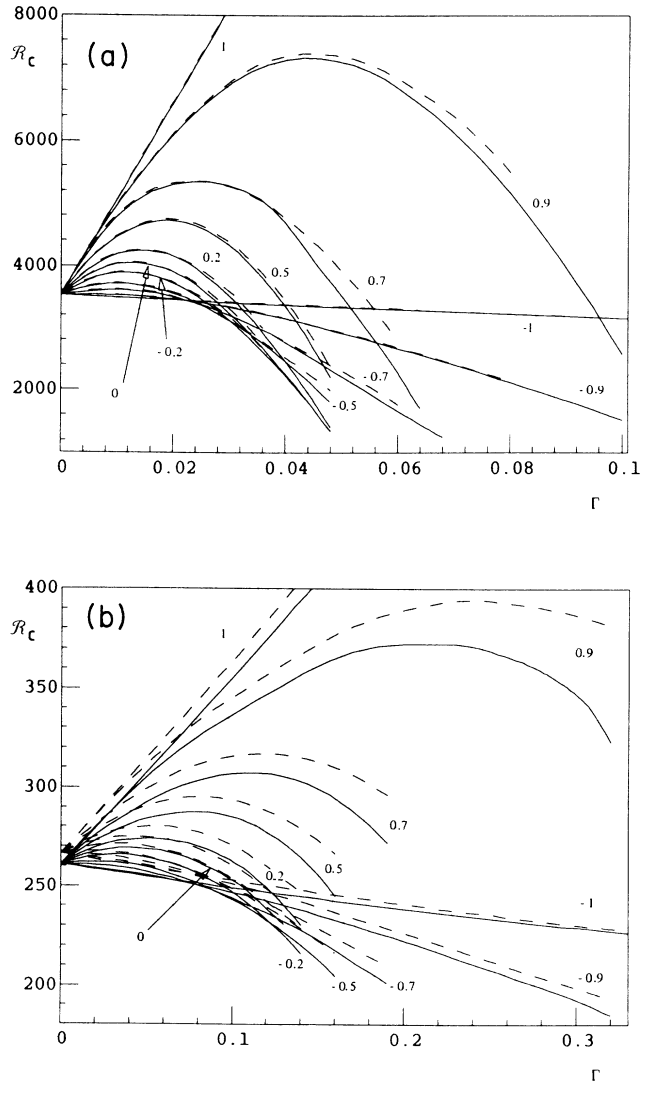

FIG. 2. Critical Reynolds number $\mathcal{R}_c$ as a function of the characteristic time Γ in the case of $\omega=0$ for (a) $a=1.0526$ and (b) $a=1.33$, for various values of A. The solid lines correspond to the stationary instability ($\nu=0, m=0$) and the dashed lines correspond to the oscillatory instability ($\nu\neq 0, m=1$).

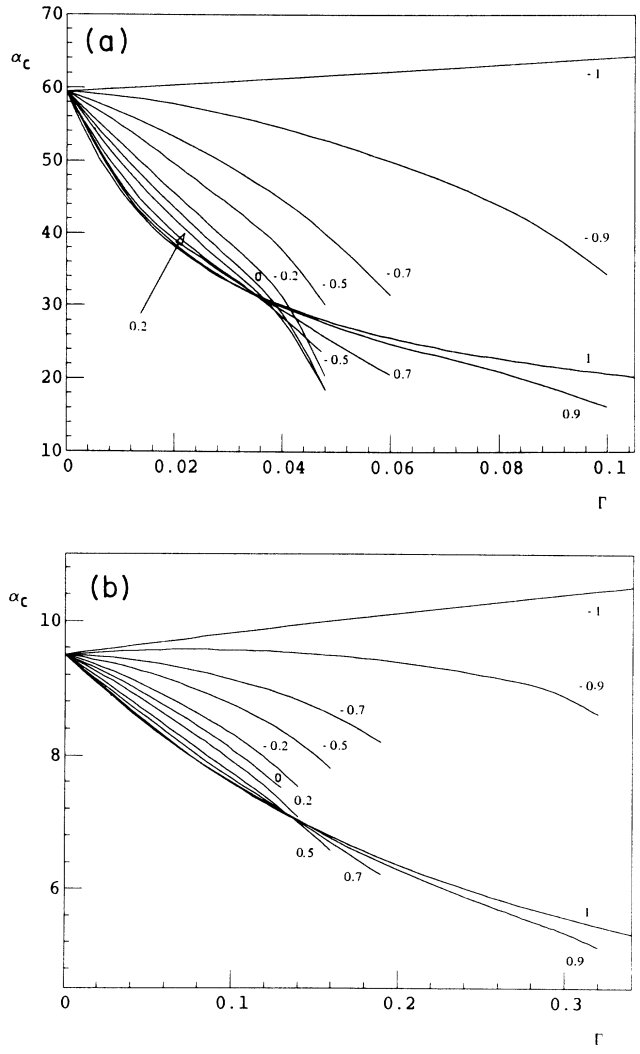

FIG. 3. Critical wave vector α_c for the stationary instability for $\omega=0$, as a function of the characteristic time Γ, for (a) $a=1.0526$ and (b) $a=1.33$ for various values of A.

and 3(b). Note, that in our case the wave vector is scaled with R_1. In order to compare the values given in Fig. 3 to the values scaled with the gap between the cylinders, they should be multiplied by the factor $1-a$. In the physically realistic range of A, i.e., $-1<A<0$, the model predicts a critical wave vector to be smaller than the one for Newtonian fluids. In some experiments no difference with the Newtonian value of the wave vector has been observed at threshold,[17,19] while in other experiments[20–22] the wave vector decreases or increases slightly. It should be pointed out however, that for small Γ, where the α_c is very close to the Newtonian value, the difference in periodicity will not be easily seen in experiment. In particular, in small aspect ratio cylinders the side boundaries will have dominating influence on the wavelength selection.

VI. CONCLUSIONS

We have solved the equations for the Couette-like flow between concentric cylinders for a large class of Maxwell models for viscoelastic fluids and have investigated its stability. It turned out that the axisymmetric steady-state solution of the basic equations does not exist for all values of the parameters A and Γ. Similar break down of the solution was already encountered in the studies of models for visoelastic fluids.[27] This breakdown of the Couette-like solution can be a sign of an existence of a different flow in this region, but most probably it points to some intrinsic problems of the rheological models.

We have found that in the region of parameters where the steady state exists, all models (except for the A very close to -1) predict stabilization of the Couette flow for small enough values for the characteristic time Γ. We conclude that the physically realistic value of A lies in the range $-1<A<0$, but more experimental data are needed to make a more precise comparison. Moreover, we have shown that in this realistic range of A there is no oscillatory instability at threshold.

ACKNOWLEDGMENTS

We want to thank G. Iooss for helpful discussions. One of us (B.J.A.Z.) acknowledges the help of the Einstein Center for Physics.

APPENDIX A

We look for a velocity field and a stress tensor depending only on the distance to one of the cylinders:

$$\vec{v}=(0,\, v_\theta^0(r),\, 0) \text{ and } \overleftrightarrow{T}=\overleftrightarrow{T}(r)^0 \text{ with } T_{ij}^0=T_{ji}^0 .$$

In this case we have

$$\nabla\vec{v}=\begin{bmatrix} 0 & \dfrac{-v_\theta^0}{r} & 0 \\ \dfrac{dv_\theta^0}{dr} & 0 & 0 \\ 0 & 0 & 0 \end{bmatrix} .$$

Substituting these expressions into Eq. (2.3) we obtain

$$T_{rr}^0=-\Gamma T_{r\theta}^0(1+A)\left[\frac{dv_\theta^0}{dr}-\frac{v_\theta^0}{r}\right], \tag{A1}$$

$$T_{\theta\theta}^0=\Gamma T_{r\theta}^0(1-A)\left[\frac{dv_\theta^0}{dr}-\frac{v_\theta^0}{r}\right], \tag{A2}$$

$$T_{r\theta}^0+\Gamma\left[\frac{dv_\theta^0}{dr}-\frac{v_\theta^0}{r}\right]\left[T_{rr}^0\frac{A-1}{2}+T_{\theta\theta}^0\frac{A+1}{2}\right]=\frac{dv_\theta^0}{dr}-\frac{v_\theta^0}{r} . \tag{A3}$$

Substitution of Eq. (A1) and (A2) into (A3) yields

$$T_{r\theta}^0=\frac{\dfrac{dv_\theta^0}{dr}-\dfrac{v_\theta^0}{r}}{1+\Gamma^2(1-A^2)\left[\dfrac{dv_\theta^0}{dr}-\dfrac{v_\theta^0}{r}\right]^2} . \tag{A4}$$

The equations for the steady state can be written now as follows:

$$\frac{dq}{dr}=\frac{(v_\theta^0)^2}{r}+\frac{1}{r\mathcal{R}}(T_{rr}^0-T_{\theta\theta}^0) , \tag{A5}$$

$$\frac{dT_{r\theta}^0}{dr}+\frac{2}{r}T_{r\theta}^0=0 . \tag{A6}$$

From Eq. (A6) it follows that

$$T_{r\theta}^0=\frac{1}{2\lambda r^2} , \tag{A7}$$

where λ is an arbitrary constant. Equation (A7) together with Eq. (A4) gives the following differential equation for v_θ^0:

$$\Gamma^2(1-A^2)\left[\frac{dv_\theta^0}{dr}-\frac{v_\theta^0}{r}\right]^2-2\lambda r^2\left[\frac{dv_\theta^0}{dr}-\frac{v_\theta^0}{r}\right]+1=0 . \tag{A8}$$

The shear rate $(dv_\theta^0/dr)-(v_\theta^0/r)$ is a solution of a second-order equation. This equation has two solution branches. Here we choose the branch corresponding to the classical Couette flow for $A=0$ and obtain

$$\frac{d}{dr}\left[\frac{v_\theta^0}{r}\right]=\frac{\lambda r}{\Gamma^2(1-A^2)}\left[1-\left[1-\frac{\Gamma^2(1-A^2)}{\lambda^2 r^4}\right]^{1/2}\right] . \tag{A9}$$

Using the Macsyma system we find the primitive of the right-hand term:

$$\frac{\lambda r^2}{2\Gamma\sqrt{1-A^2}}\left\{r^2-\left[\frac{\lambda^2 r^4}{\Gamma^2(1-A^2)}-1\right]^{1/2}-\Gamma\sqrt{1-A^2}\arctan\left[\left[\frac{\lambda^2 r^4}{\Gamma^2(1-A^2)}-1\right]^{1/2}\right]+\mu\right\}.$$

This solution depends on two arbitrary constants λ and μ. From the last expression Eq. (3.2) for v_θ^0 easily follows.

APPENDIX B

Inserting expressions (4.1) into the constitutive equation, Eqs. (2.3a), and linearizing around the perturbations, one obtains the following set of equations:

$$\eta_{rr}+\Gamma[(\sigma+imv_\theta^0/r)\eta_{rr}-2v_\theta^0\eta_{r\theta}/r+(\partial_r T_{rr}^0)u_r-2T_{r\theta}^0 u_\theta/r]$$
$$+\Gamma\{(A+1)[(\partial_r v_\theta^0)\eta_{r\theta}+T_{rr}^0\partial_r u_r+T_{r\theta}^0\partial_r u_\theta]+(A-1)[-v_\theta^0\eta_{r\theta}/r+T_{rr}^0\partial_r u_r+T_{r\theta}^0(imu_r-u_\theta)/r]\}=2\partial_r u_r\ , \tag{B1}$$

$$\eta_{r\theta}+\Gamma[(\sigma+imv_\theta^0/r)\eta_{r\theta}+(\eta_{rr}-\eta_{\theta\theta})v_\theta^0/r+(\partial_r T_{r\theta}^0)u_r+(T_{rr}^0-T_{\theta\theta}^0)u_\theta/r]$$
$$+\tfrac{1}{2}\Gamma\{(A+1)[(\partial_r v_\theta^0)\eta_{\theta\theta}-v_\theta^0\eta_{rr}/r+T_{rr}^0(imu_r-u_\theta)/r+T_{r\theta}^0(imu_\theta+u_r)/r+T_{r\theta}^0\partial_r u_r+T_{\theta\theta}^0\partial_r u_\theta]$$
$$+(A-1)[(\partial_r v_\theta^0)\eta_{rr}-v_\theta^0\eta_{\theta\theta}/r+T_{r\theta}^0\partial_r u_r+T_{\theta\theta}^0(imu_r-u_\theta)/r+T_{rr}^0\partial_r u_\theta+T_{r\theta}^0(imu_\theta+u_r)/r]\}$$
$$=(imu_r-u_\theta)/r+\partial_r u_\theta\ , \tag{B2}$$

$$\eta_{rz}+\Gamma[(\sigma+imv_\theta^0 r)\eta_{rz}-v_\theta^0\eta_{\theta z}/r]+\tfrac{1}{2}\Gamma\{(A+1)[(\partial_r v_\theta^0)\eta_{\theta z}+T_{rr}^0 i\alpha u_r+T_{r\theta}^0 i\alpha u_\theta]$$
$$+(A-1)[-v_\theta^0\eta_{\theta z}/r+T_{rr}^0\partial_r u_c+T_{r\theta}^0 imu_z/r]\}=i\alpha u_r+\partial_r u_z\ , \tag{B3}$$

$$\eta_{\theta\theta}+\Gamma[(\sigma+imv_\theta^0/r)\eta_{\theta\theta}+2v_\theta^0\eta_{r\theta}/r+(\partial_r T_{\theta\theta}^0)u_r+2T_{r\theta}^0 u_\theta/r]$$
$$+\Gamma\{(A+1)[-v_\theta^0\eta_{r\theta}/r+T_{r\theta}^0(imu_r-u_\theta)/r+T_{\theta\theta}^0(imu_\theta+u_r)/r]$$
$$+(A-1)[(\partial_r v_\theta^0)\eta_{r\theta}+T_{r\theta}^0\partial_r u_\theta+T_{\theta\theta}^0(imu_\theta+u_r)/r]\}=2(imu_\theta+u_r)/r\ , \tag{B4}$$

$$\eta_{\theta z}+\Gamma[(\sigma+imv_\theta^0/r)\eta_{\theta z}+v_\theta^0\eta_{rz}/r]\tfrac{1}{2}\Gamma\{(A+1)[-v_\theta^0\eta_{rz}/r+T_{r\theta}^0 i\alpha u_r+T_{\theta\theta}^0 i\alpha u_\theta]$$
$$+(A-1)[(\partial_r v_\theta^0)\eta_{rz}+T_{r\theta}^0\partial_r u_z+T_{\theta\theta}^0 imu_z/r]\}=i\alpha u_\theta+imu_z/r\ , \tag{B5}$$

$$\eta_{zz}+\Gamma(\sigma+imv_\theta^0/r)\eta_{zz}=2i\alpha u_z\ . \tag{B6}$$

Similarly the incompressibility condition, Eq. (2.3b), takes the form

$$\partial_r u_r+u_r/r+imu_\theta/r+i\alpha u_z=0\ . \tag{B7}$$

Finally the Navier-Stokes equation, Eq. (2.3c), gives, after linearization,

$$\sigma u_r+v_\theta^0(imu_r-2u_\theta)/r+\partial_r\psi$$
$$=\mathcal{R}^{-1}[\partial_r\eta_{rr}+im\eta_{r\theta}/r+i\alpha\eta_{rz}+(\eta_{rr}-\eta_{\theta\theta})/r]\ , \tag{B8}$$

$$\sigma u_\theta+u_r(\partial_r+1/r)v_\theta^0+v_\theta^0 imu_\theta/r+im\psi/r$$
$$=\mathcal{R}^{-1}[\partial_r\eta_{r\theta}+im\eta_{\theta\theta}/r+i\alpha\eta_{\theta z}+2\eta_{r\theta}/r]\ , \tag{B9}$$

$$\sigma u_z+v_\theta^0 imu_z/r+i\alpha\psi$$
$$=\mathcal{R}^{-1}[\partial_r\eta_{rz}+im\eta_{\theta z}/r+i\alpha\eta_{zz}+\eta_{rz}/r]\ . \tag{B10}$$

Equations (B1)–(B10) do not contain the derivatives with respect to r of $\eta_{\theta\theta}$, $\eta_{\theta z}$, and η_{zz}. Consequently $\eta_{\theta\theta}$, $\eta_{\theta z}$, and η_{zz} can be calculated from Eqs. (B4), (B5), and (B6) and substituted in the remaining set of equations. Similarly, η_{rr} can be calculated from Eq. (B1). By taking a derivative with respect to r of Eqs. (B1) and (B7) and substituting for $\partial_r^2 u_r\partial_r\eta_{rr}$ can also be eliminated from Eq. (B8). In this way one finds a set of six linear equations for u_r, u_θ, u_z, $\eta_{r\theta}$, η_{rz}, and ψ and its first derivatives with respect to r. This set of equations can be readily put into a form presented in Eq. (4.2).

*Present address: Institüt für Festköperforschung, Kernforschungsanlage Jülich (KFA), D-5170 Jülich, Federal Republic of Germany.

[1]A. S. Lodge, *Elastic Liquids* (Academic, New York, 1964).
[2]R. B. Bird, R. C. Armstrong, and O. Hassager, *Dynamics of Polymeric Liquids* (Wiley, New York, 1977).
[3]J. D. Ferry, *Viscoelastic Properties of Polymers* (Wiley, New York, 1980).
[4]For example, see Ref. 2, p. 90.
[5]F. H. Garner and A. H. Nissan, Nature **158**, 634 (1946).
[6]K. Weissenberg, Nature **199**, 310 (1947).
[7]Reference 2, p. 92.

[8]J. Meissner, Rheol. Acta **10**, 230 (1971).
[9]Reference 1, p. 236.
[10]J. C. Maxwell, Philo. Trans. R. Soc. London, Ser. A **157**, 49 (1861).
[11]J. G. Oldroyd, Proc. R. Soc. London, Ser. A **200**, 523 (1950).
[12]J. G. Oldroyd, Proc. R. Soc. London, Ser. A **245**, 278 (1958).
[13]J. S. Petrie and M. M. Denn, AIChE J. **22**, 209 (1976).
[14]R. H. Thomas and K. Walters, J. Fluid Mech. **18**, 33 (1964).
[15]D. W. Beard, M. H. Davis, and K. Walters, J. Fluid Mech. **24**, 321 (1966).
[16]Chan Man Fong, Rheol. Acta **4**, 37 (1965).
[17]H. Rubin and C. Elata, Phys. Fluids **9**, 1929 (1966).
[18]M. M. Denn and J. Roisman, AIChE J. **15**, 454 (1969).
[19]J. W. Hayes and J. F. Hutton, Prog. Heat Transfer **5**, 195 (1970).
[20]Z. S. Sun and M. M. Denn, AIChE J. **18**, 1010 (1972).
[21]W. M. Jones, D. M. Davies, and M. C. Thomas, J. Fluid Mech. **60**, 19 (1973).
[22]G. S. Beavers and D. D. Joseph, Phys. Fluids **17**, 650 (1974).
[23]B. J. A. Zielinska, *Convection in Viscoelastic Fluids, Proceedings of the Workshop on Propagation in Nonequilibrium Systems, Les Houches, France, 1987,* edited by J. E. Wesfried *et al.* (Springer, Heidelberg, 1988).
[24]P. Chossat and G. Iooss, Jpn. J. Appl. Math. **2**, 37 (1985).
[25]Y. Demay and G. Iooss, J. Méc., Spec. Suppl., 193 (1984).
[26]J. D. Griffiths and R. H. Thomas, J. Méc. **5**, 101 (1966).
[27]D. D. Joseph, M. Renardy, and J. C. Saut, Arch. Rat. Mech. Anal. **87**, 213 (1985).